Creep and Relaxation Behaviour of Mg-Al based Die cast Alloys AZ91 and AE44

Dipl.-Ing. Gerhard Gerstmayr, Dr. Heinz Leitner, Prof. Dr. Wilfried Eichlseder

University of Leoben, Department of Product Engineering
Franz-Josef Str. 18
8700, Leoben

Abstract

The creep behaviour of die cast magnesium alloys AZ91 and AE44 was investigated using constant uniaxial tensile load creep testing in the temperature range from 120°C to 180°C. At high stress levels AZ91 was found to have better creep resistance meaning lower primary and secondary creep rates. However, when decreasing load to a certain load range the superior creep properties change from AZ91 to AE44 nearly independent from temperature.

The characteristic creep curves of both alloys at a certain load and temperature level were modelled using a power law on basis of Norton and calculated creep curves in FE-Solver ABAQUS showed good correlation to experimental creep test data. Pure magnesium relaxation calculations on basis of creep behaviour were compared to static relaxation test results of a bolted joint. The experimental relaxation curves showed good correlation to simulation results concerning progress and characteristics of relaxation.

Introduction

Increasing safety-requirements as well as growing customer demands for comfort cause a significant increase of weight in all classes of automobile industry. Consequently, more effective and efficient lightweight design has become more important to face challenges like emission reduction and lower fuel consumption. A 10 % reduction in vehicle weight leads to a reduction in fuel-consumption of between 0,3 and 0,5 l/100km [1].

Mg die cast alloys offer considerable potential for vehicle weight reduction in comparison to traditional construction materials like aluminium and steel. Its low density of about 1,8 g/cm^3 leads to a high specific strength. Moreover, its good workability and recyclability make Mg alloys an attractive light weight material in automotive industry [2]. Mg-Al alloys such as AZ91 are used because of superior castability and good balance of strength and ductility. However, this alloy exhibits poor high temperature properties and there occurs a rapid degradation in mechanical properties, especially creep properties, when a temperature of 120°C is exceeded [3].

Power-train components like gear box housings may reach temperatures of 150°C in service and therefore Mg die cast alloys with superior elevated temperature properties are needed. A promising rare earth containing Mg-Al alloy is AE44 (Mg-4%Al-4%RE, composition in wt.%). Comprehensive investigations on the alloy AE42 [4] showed that the superior creep resistance exhibited by AE42 compared with conventional Mg-Al based alloys like AZ91 is caused by the suppression of $Mg_{17}Al_{12}$ during solidification due to the preferential formation of intermetallic stable Al_xRE_y compounds.

This paper investigates and compares the creep behaviour of AZ91 and AE44 over a wide range of combined thermal and mechanical loadings relevant for power-train applications. Based on comprehensive experimental creep tests, the application limits of AZ91 for components which are subjected to elevated temperatures are discussed. Fundamental micro structural investigations are made to explain the creep behaviour. Furthermore, the effect of the creep behaviour of the investigated Mg-alloys AZ91 and AE44 on the relaxation behaviour of a light metal bolted joint is presented and discussed.

Creep

Normally, data from constant load creep tests is displayed as a strain versus time plot (figure 3a).

The minimum creep strain rate $\dot{\varepsilon}$ is a function of stress and temperature and remains constant over a certain range of strain. It is the most important parameter when creep resistance of different materials is compared [5, 2].

For most metals including Mg-Al alloys the relationship of the secondary creep rate and stress can be described by a power law. A general form is

$$\dot{\varepsilon}_s = A \cdot \sigma^n \cdot \exp(-Q_c /(R \cdot T)) .$$

Where A is a constant, Q_c is the activation energy for creep, n is the stress exponent, σ is the applied stress, T is absolute temperature and R is the gas constant [2, 6].

Experimental

Samples in shape of a plate with two bolting spots were produced by die casting using a cold chamber machine (figure 1a). The thickness of the quadratic castings is 12 mm with an edge length of 100 mm. The specimens for uniaxial tensile creep testing were taken from the edges of the plate (figure 1b). At this position, good mechanical properties due to high cooling rates and low porosity are expected.

Figure 1: Die cast samples with gate system (a); position of specimen taking for creep tests (b)

The chemical composition of the two investigated high pressure die cast alloys is listed in table 1.

Table 1: Chemical composition of die cast alloys AZ91 and AE44

Alloy	Al	Zn	Mn	Cu	Fe	Si	RE
AZ91	8,7	0,8	0,1	0,08	<0,002	0,03	0,2
AE44	3,7	0,01	0,2	0,003	<0,002	0,03	3,9

The used creep test rig was designed at the department for product engineering. A loading system consisting of lever and weights was chosen. The creep test is made in an Instron heat chamber (figure 2a). The clamping of the creep specimen is form-fit with a M12x1,5 thread. The creep strain is measured by an extensometer. Three thermocouples Typ K at the specimen guarantee a homogenous temperature field over the entire length of the testing cross section (figure 2b).

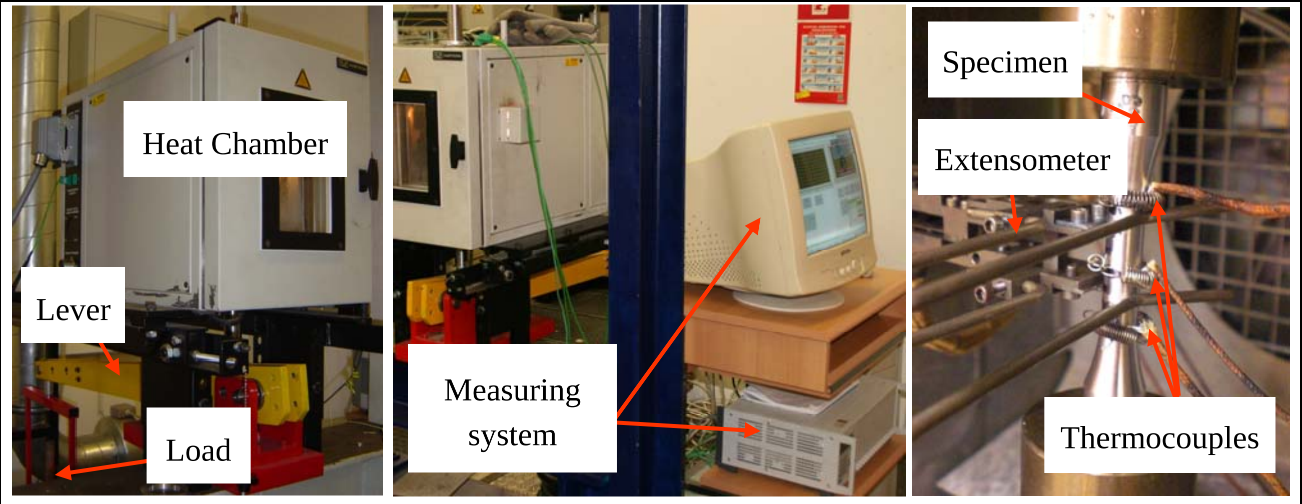

Figure 2: Test rig used for constant load tensile creep tests (a), creep specimen with extensometer and thermocouples (b)

After reaching constant temperature, the specimen was kept unloaded at constant temperature for 15 minutes to ensure a homogenous temperature distribution. Subsequently the data measurement system (Spider 8) was started and the weight was applied. This procedure was repeated carefully to avoid any scattering of test results due to varying temperature and dwell time.

In table 2, the test matrix is shown.

Table 2: Test matrix of tensile creep tests on AZ91 and AE44

Alloy	AZ91				AE44			
Stress [MPa]	Temperature [°C]				Temperature [°C]			
	120	135	150	180	120	135	150	180
65		X	X			X	X	
82	X		X	X	X		X	X
85		X				X		
89			X		X		X	
97	X		X		X		X	
112	X		X		X		X	
127	X				X			

In figure 3b the creep curves of both investigated Mg-alloys AZ91 and AE44 at a temperature of 120°C at different load levels are displayed. To compare the two alloys, one has to consider the full line (AE44) with the slashed line (AZ91) at a certain load level. At the investigated high load levels 127 MPa and 112 MPa, AZ91 exhibits significantly better creep properties than AE44, noticeable by lower minimum creep rates (slope of tangent in steady-state area) and higher rupture times. At the load level of 97 MPa, AZ91 again reveals a higher rupture time of more than 400 hours in comparison to approx. 50 hours of AE44.

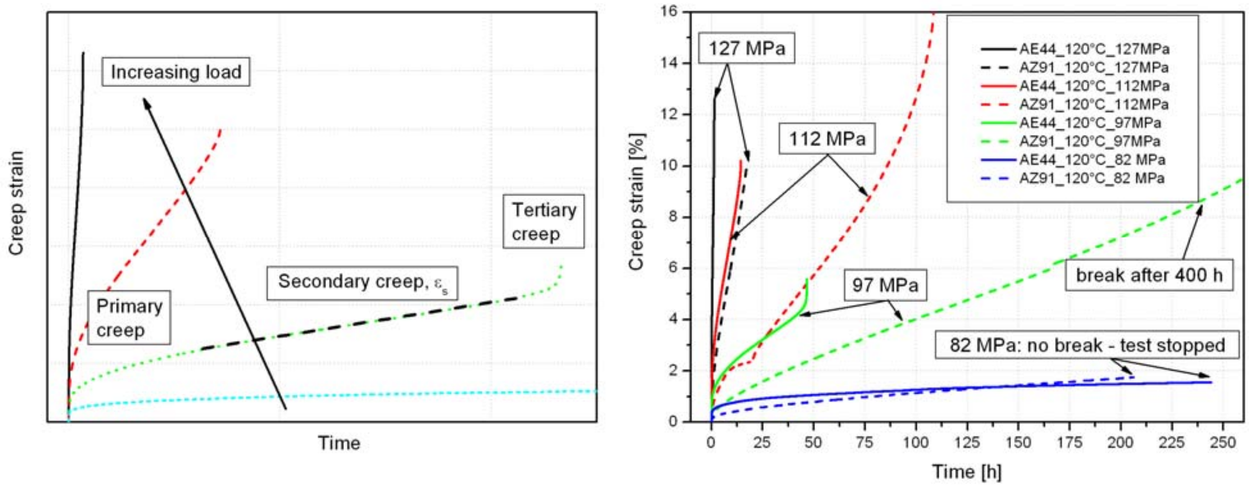

Figure 3: Typical shape of creep curves from constant load creep tests (a); creep curves of AZ91 and AE44 at 120°C (b)

However, the minimum creep rates of both alloys are similar. If the load level is decreased to 82 MPa, AE44 reveals better creep properties, meaning lower minimum creep rates in the steady-state area than AZ91, for the first time.

A significant difference in the creep behaviour of AZ91 and AE44 is identifiable in the primary creep area. First, the amount of creep strain caused by load application, consisting of elastic and plastic strain, is higher for the alloy AE44 in comparison to AZ91 (figure 4b). The reason for this is that AE44 reveals a lower yield strength which leads to earlier plastic deformation and consequently to higher spontaneous strains when load is applied. The influence of the different material strength of the two alloys on the strain when the load is applied grows with increasing load level according to quasistatic tensile test data as can be seen in figure 4a.

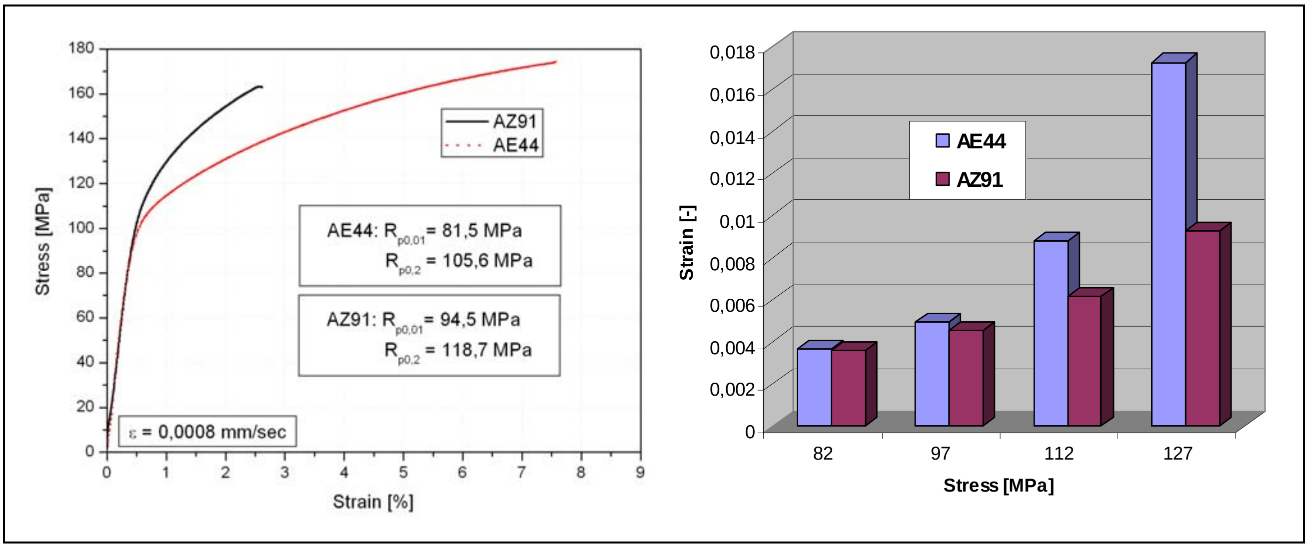

Figure 4: Quasistatic tensile test data of AZ91 and AE44 (a), difference in total strain due to load application between AZ91 and AE44 (b)

Secondly, short after the load is applied the progress of the creep strain differs significantly between AZ91 and AE44 (figure 5a). The alloy AE44 reveals a high creep rate in the beginning which decreases rapidly after a certain period of time depending on stress and temperature level. On the contrary AZ91 exhibits a strong decrease of creep rate immediately after load application. Obviously, hardening effects due to increasing dislocation density occur stronger in AZ91 than in AE44.

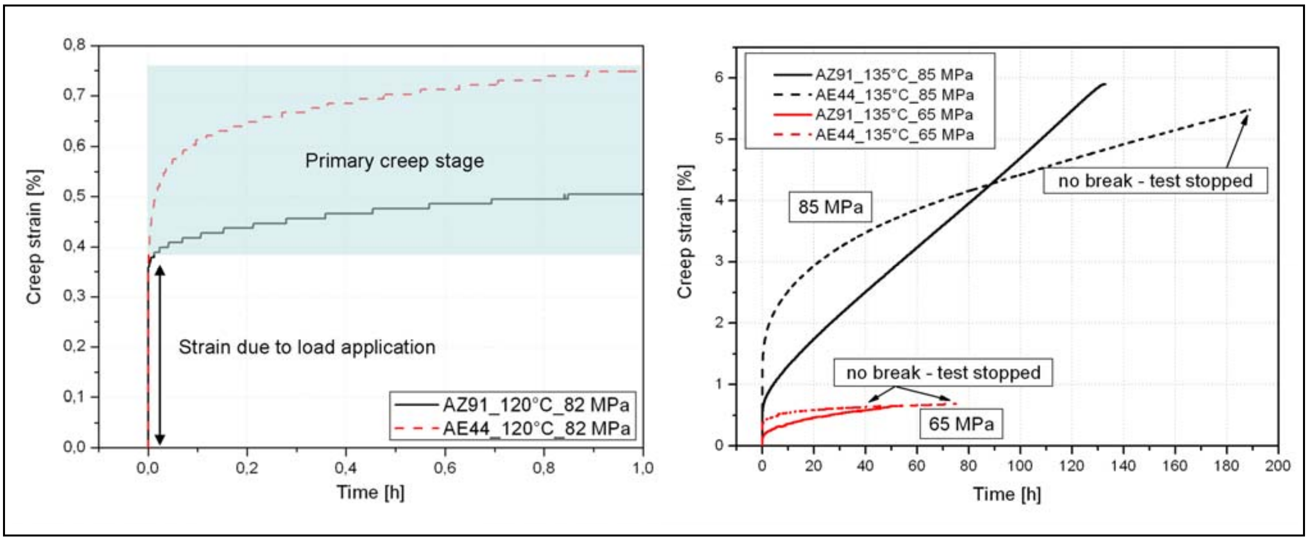

Figure 5: Difference in primary creep stage between AZ91 and AE44 after load application (a), creep curves of AZ91 and AE44 at 135°C (b)

Figure 5b shows the creep curves of AZ91 and AE44 at a temperature of 135°C for two different load levels. In [1], a load combination of 85 MPa and 135°C was chosen as an example of a gearbox housing load case. At both load levels AE44 shows better creep properties than AZ91. The same tendency as at 120°C can be observed regarding primary as well as secondary creep rates of AZ91 and AE44. At both investigated load levels AZ91 reveals lower primary creep rates. However, higher secondary creep rates in comparison to AE44 lead to an intersection point at both load levels. It can be assumed that similar to 120°C AZ91 will reveal superior creep properties when load is increased to a certain extent.

At a temperature of 150°C, five different load levels in the range from 112 MPa to 65 MPa were investigated. Figure 6a shows the creep behaviour of AZ91 and AE44 for high loads. At 112 MPa as well as 97 MPa AZ91 exhibits superior creep properties, meaning lower primary and secondary creep rates than AE44. When load is decreased to 89 MPa the two alloys show similar secondary creep rates analogous to 120°C. However, due to lower primary creep rates of AZ91 the resulting creep behaviour is better than AE44. At a load level of 82 MPa, AE44 exhibits better creep resistance than AZ91 for the first time at this temperature level. An intersection point due to higher primary but lower secondary creep rates occurs as described before. The same behaviour can be observed when the load is further decreased to 65 MPa.

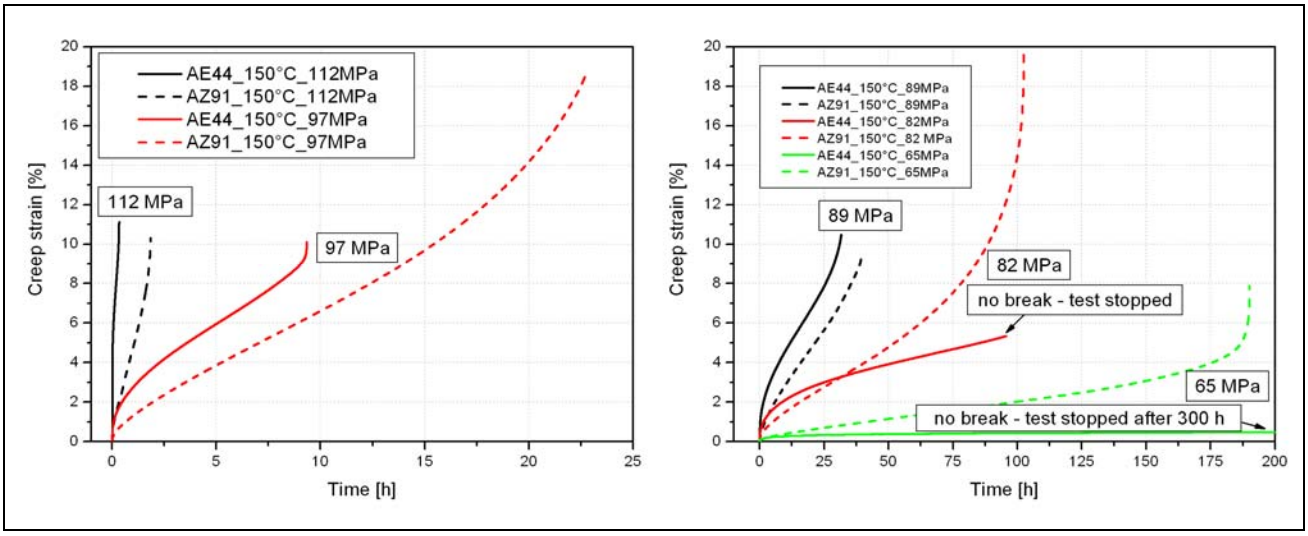

Figure 6: Creep curves of AZ91 and AE44 at 150°C at high load levels (a), at low load levels (b)

At a temperature of 180°C only the load level 82 MPa was investigated as can be seen in figure 7a. Similar to the temperature levels 120°C and 150°C, the rare-earth containing alloy AE44 shows lower secondary creep rates than AZ91.

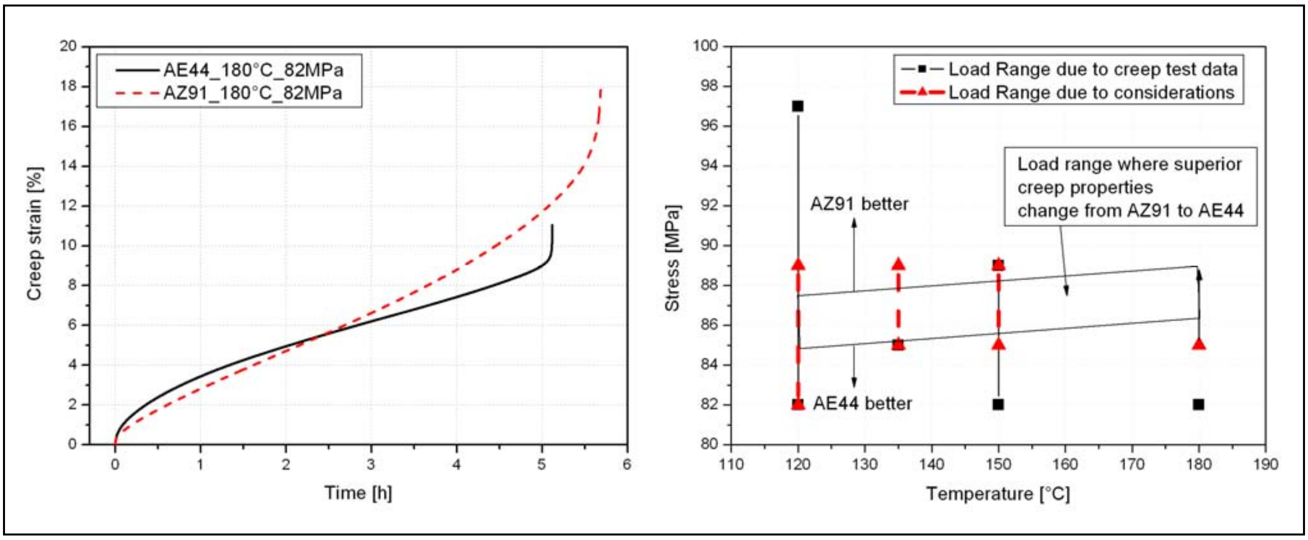

Figure 7: Creep curves of AZ91 and AE44 at 180°C (a), definition of the load range where superior creep properties change from AZ91 to AE44 (b)

It seems that there exists a certain load level or load range exists which is nearly independent from the temperature level where superior creep properties change from one alloy to the other. For high load levels in the range of the yield strength, the alloy AZ91 reveals lower minimum creep rates than AE44. This difference in the secondary creep rate becomes smaller with decreasing load down to a certain load level where AE44 reveals superior creep resistance, meaning lower secondary creep rates.

At a temperature of 120°C, the load range where the superior creep resistance changes from AZ91 to AE44 lies between 82 MPa and 97 MPa according to experimental creep data. Due to lack of creep tests within this range, a more detailed specification is not possible. At a temperature of 135°C, the load level has to be higher than 85 MPa. At 150°C the possible range is between 82 MPa and 89 MPa.

The following thoughts may help to define the load range more exactly. Numerous investigations proved that AE44 reveals better high temperature properties than AZ91. Therefore, it can be assumed that the load level where the alloy AE44 reveals better creep properties than AZ91 increases with rising temperature. As a consequence the load range at a temperature above 135°C is at least 85 MPa and less than 89 MPa up to a temperature of 150°C. The upper level of the load range at 180°C is estimated with about 90 MPa (figure 7b).

Microstructural investigations

The main constituents of the microstructure of the die cast alloys AZ91 and AE44 are shown in figure 8 and figure 10. The microstructure of AZ91 consists of a primary solidified α-Mg solid solution and intergranular particles of β-$Mg_{17}Al_{12}$ phase. The dark surrounding of the $Mg_{17}Al_{12}$ phase is an Al rich supersaturated α-Mg sold solution which forms last during solidification sequence [6, 2]. These segregations are composed due to a low diffusion of Al in Mg. SEM-EDX analysis showed that the Al-content in the first solidified solid solution is about 2,7 % and increases up to 10 % in the dark supersaturated areas surrounding the $Mg_{17}Al_{12}$ phase.

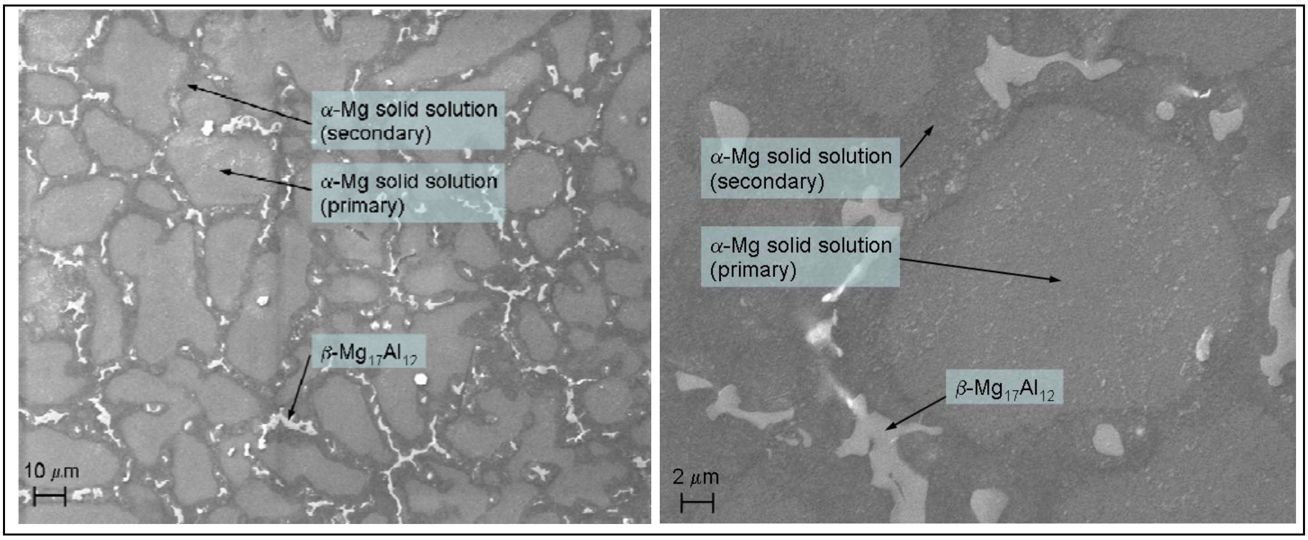

Figure 8: Microstructure of die cast alloy AZ91

It was found by [2] and [6] that the major reason for the moderate creep resistance of AZ91 is because of the thermal instability of the Al-rich supersaturated areas of α-Mg when subjected to elevated temperatures. Discontinuous as well as continuous precipitation of β-$Mg_{17}Al_{12}$ occurs during creep testing emanating from grain boundaries and intergranular β-$Mg_{17}Al_{12}$ grains.

Using dark field light microscopy the β-$Mg_{17}Al_{12}$ phase appears as bright edged areas (figure 9a). After creep testing at 120°C for 170 hours significant micro structural changes are visible (figure

9b). β-precipitations out of the supersaturated α-Mg solid solution are identifiable. As a consequence a lower amount of supersaturated α-Mg solid solution is left. Due to the elevated temperatures the diffusion of Al in Mg is higher and after nucleation, the β-precipitations grow by withdrawing Al from the surroundings. Therefore, no sharp edged precipitation areas are noticeable, but merely groups of precipitations in the shape of dots.

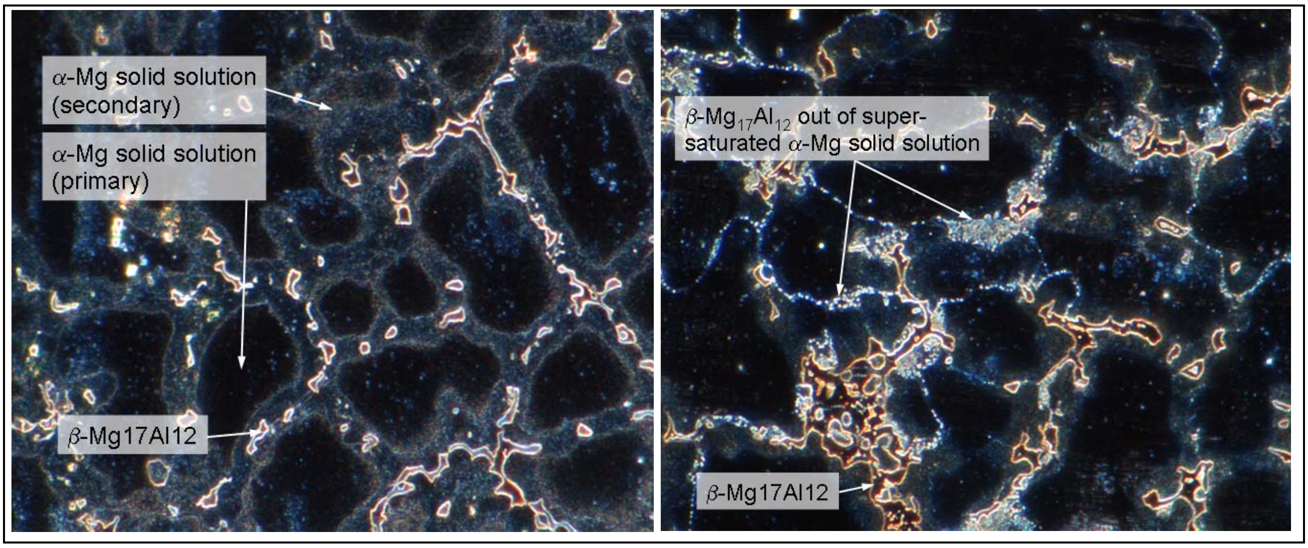

Figure 9: Microstructure of AZ91 in dark field microscopy as cast (a), after creep testing (b)

The microstructure of AE44 consists of α-Mg solid solution, a lamellar eutectic consisting of α-Mg solid solution and Al_xRE_y precipitations and single Al_xRE_y precipitations (figure 10). [6] and [4] investigated the alloy AE42 and found no β-$Mg_{17}Al_{12}$ phase because of the preferential formation of intermetallic thermally stable Al_xRE_y compounds. [6] found no precipitations of β-$Mg_{17}Al_{12}$ during creep testing due to the low amount of supersaturated α-Mg solid solution in comparison to AZ91.

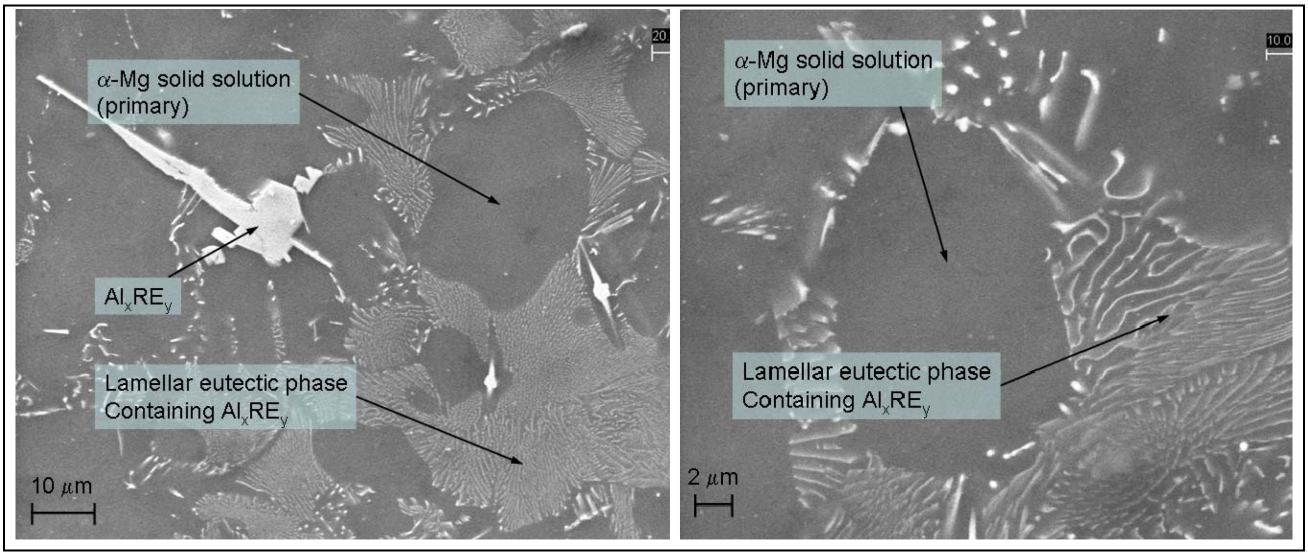

Figure 10: Microstructure of AE44

When comparing the shape of a typical creep curve of AZ91 and AE44 it can be seen that AZ91 (figure 6) reveals no distinctive steady-state area but merely just a short area of constant creep rate which ends in a significantly long tertiary stage with gradually increasing creep rate. The constant creep rate in the steady-state area is based on an equilibrium of hardening and softening effects. The significant micro structural changes during creep testing, meaning gradually precipitating, could be an explanation for the above mentioned characteristic shape of AZ91 creep curves.

Modelling of creep behaviour

A power law model based on Norton it its time hardening form was used to describe the primary as well as the secondary part of the creep curve. This model is implemented in the FE-Solver ABAQUS 6.7.

$$\dot{\varepsilon} = A \cdot \sigma^n \cdot t^m$$

Where $\dot{\varepsilon}$ is the uniaxial equivalent creep strain rate, sigma is the uniaxial equivalent stress, t is the total time and A, n and m are defined as functions of temperature. After bringing the equation it its differential form

$$\partial \dot{\varepsilon} = A \cdot \sigma^n \cdot t^m \partial t$$

and integrating both sides of the equation, the creep strain versus time plots can be described.

$$\varepsilon = \frac{1}{(m+1)} \cdot A \cdot \sigma^n \cdot t^{(m+1)}$$

For physically reasonable creep behaviour, the constants A and n must be positive and m must be in the range $-1 < m \leq 0$. The constants A, n and m were determined analytically and optimised by means of Excel-Solver for one representing creep curve of both alloys AZ91 and AE44. Figure 11a shows plots of pure creep strain versus time for AZ91 and AE44 at 120°C and an uniaxial tensile load of 82 MPa without elastic-plastic strain due to load application. Due to limited testing time the tests were aborted without rupture after reaching about 200 hours. It is reasonable to model only the primary and secondary creep stage because when reaching tertiary creep stage in service, the component will probably lose functionality.

First, a duration of 10 hours was modelled to estimate the influence of the primary creep behaviour on the resulting relaxation behaviour (figure 11b).

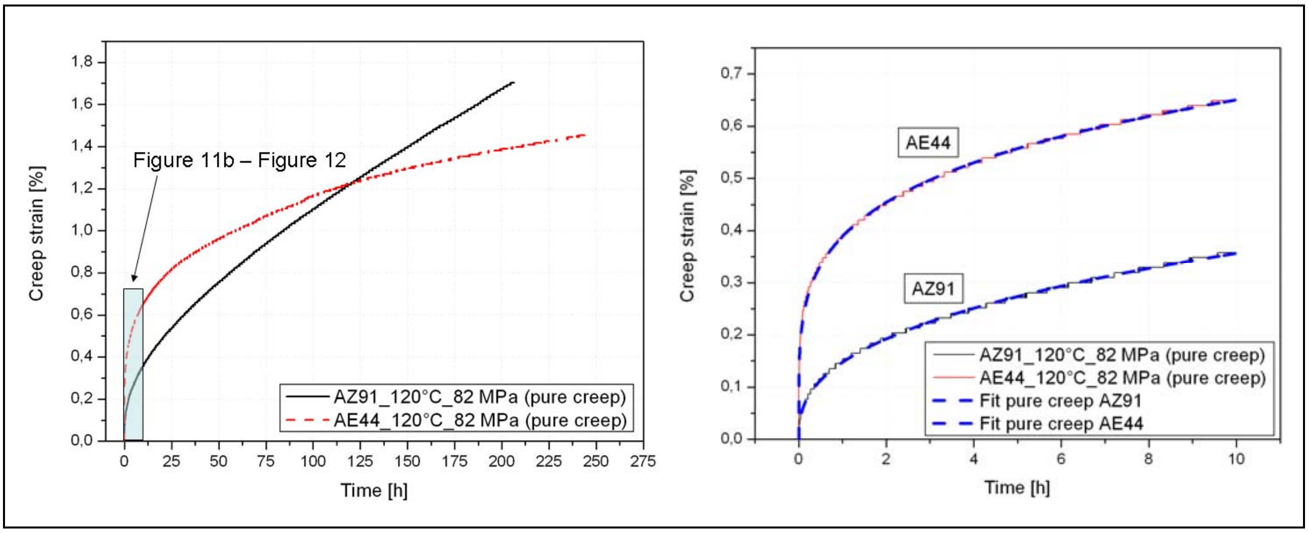

Figure 11: Creep curves of die cast alloys at 120°C and 82 MPa (a), modelling of creep curves (b)

The creep curves of AZ91 and AE44 for the first 10 hours can be modelled exactly with the before described power law. Adding the elastic-plastic strain due to load application leads to the dotted lines in figure 12a.

In the next step, the experimental creep tests are simulated in ABAQUS, using a two step model for load application and subsequent creep. The determined parameter A, n and m are implemented in ABAQUS. According to the experimental test procedure, the displacement of a specified node, representing the blade of the used extensometer, was measured and calculated to strain.

The creep curve of AZ91 can be simulated exactly by ABAQUS, whereas a discrepancy between the experimental and the simulated creep curve occurs for AE44.

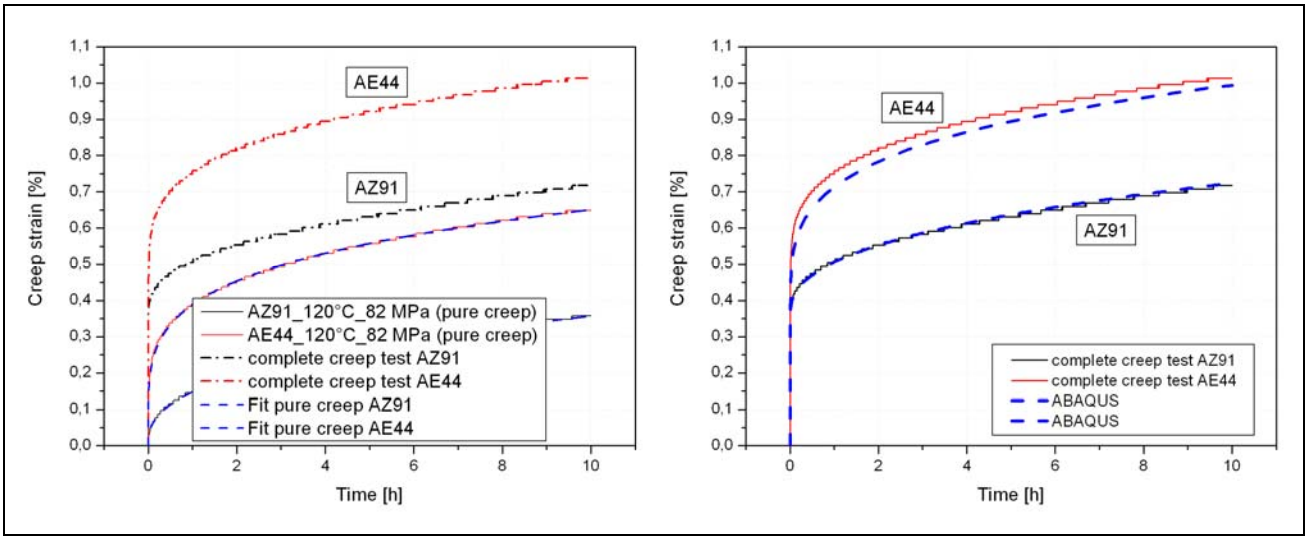

Figure 12: Experimental creep test curves including elastic-plastic strain due to load application and creep strain (a), calculated creep curves with FE-solver ABAQUS (b)

Influence of creep behaviour on relaxation of a bolted joint

Is the strain in a metal kept constantly at elevated temperatures, stresses are reduced with progressing time due to creep mechanisms. This procedure is called relaxation [7].

Current solutions that are frequently used for magnesium bolt connections are steel bolts with aluminium cups (or other head encapsulations) or metric aluminium bolts in EN AW 6056 alloy [8, 9]. An essential specific value regarding leak tightness or functionality in general is the bolt load of a bolted joint. The influence of the investigated creep characteristics of AZ91 and AE44 on relaxation in general is discussed. Subsequently a qualitative comparison with experimental test results is made.

Basic simulations

A specified displacement was applied that causes a linear elastic stress of about 80 MPa to gain an initial stress value in the range of the modelled creep curves. The sum of the reaction forces of all nodes in the centre of the modelled specimen versus time is shown in figure 13a. During applying the specified displacement in the first step, plastic deformations occur in the alloy AE44 due to exceeding yield strength, whereas the alloy AZ91 still shows linear elastic behaviour after displacement application. Consequently the initial value of reaction forces of AZ91 is higher.

After starting the creep step the loss of reaction force of AE44 is more rapid due to higher primary creep strain rates as can be seen in figure 13a. However, with increasing time the difference in reaction force between AZ91 and AE44 becomes smaller.

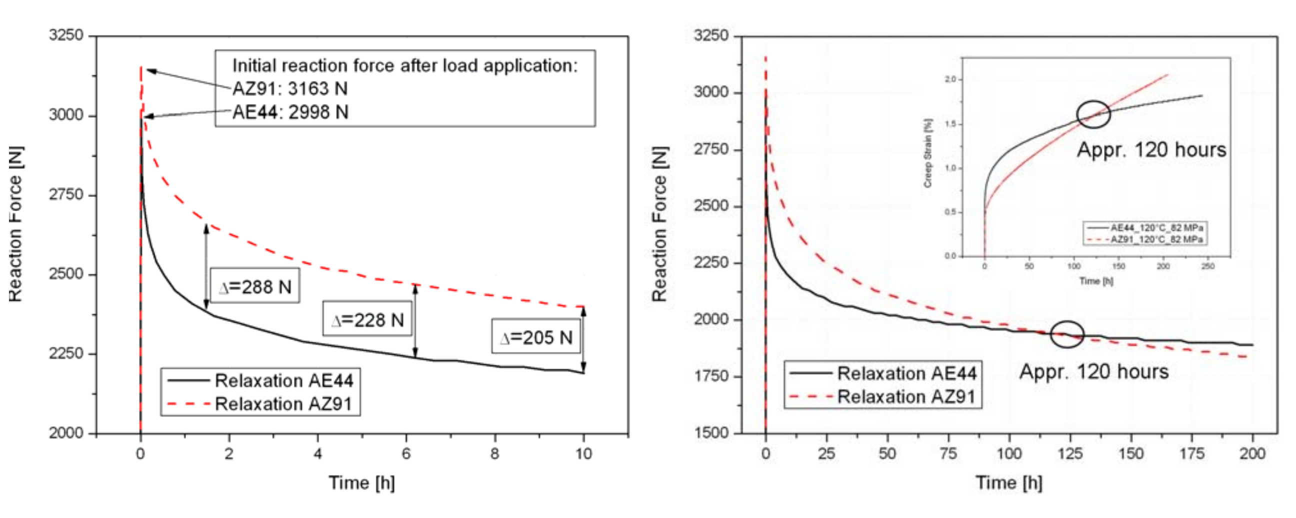

Figure 13: Relaxation curve of AZ91 and AE44 for 10 hours (a), for 200 hours (b)

When modelling a test duration of 200 hours, the relaxation curves of AZ91 and AE44 show a good correlation to the creep curves. Gradually decreasing creep strain rates of AE44 after high initial primary creep rates at the beginning of the test cause proceeding decreasing relaxation rates. The intersection point at approximately 120 hours for creep and relaxation proves good correlation between calculated relaxation and experimental creep data.

Relaxation test results

To verify the above made considerations, static relaxation tests of a Mg light metal bolted joint subjected to a temperature of 120°C are performed. The joint was bolted with a thread forming trilobular steel bolt TT2000 M8x60 with a specified tightening procedure based on experimental tests. Due to a fixed bolt length, a sleeve made of steel was used to guarantee a defined thread engagement length of about three times the nominal diameter of the bolt (figure 14). The bolt load was measured with a calibrated temperature compensated load cell of the type KALIBER. Temperature measurement was made by a thermocouple type K. For data acquisition a measurement amplifiers Spider 8 with the software CATMAN was used.

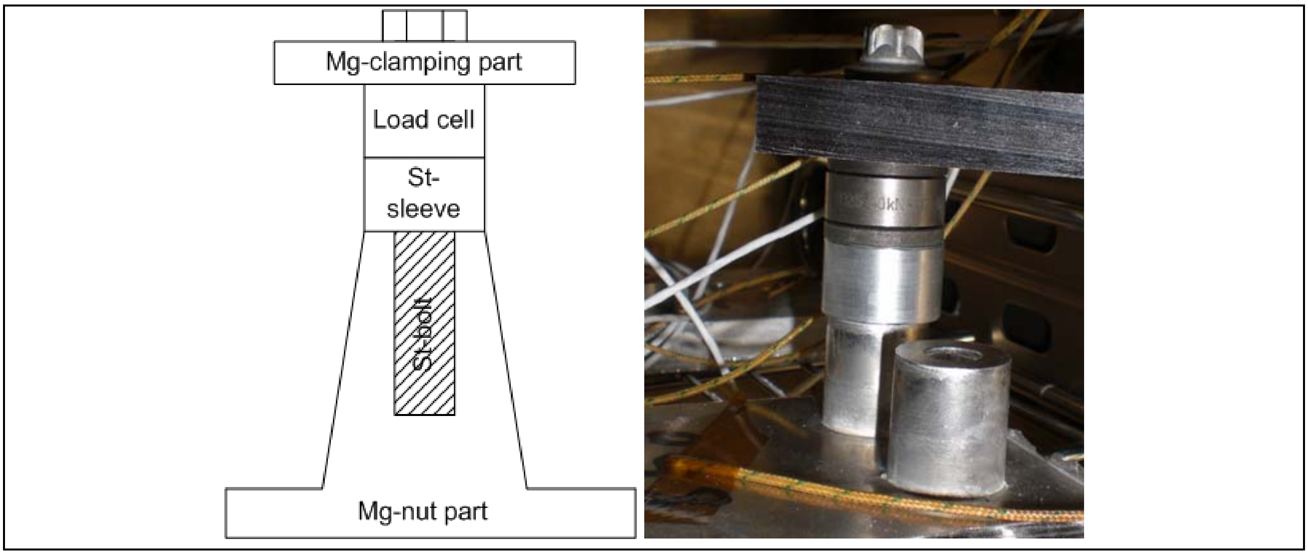

Figure 14: Investigated light metal bolted joint for relaxation tests

Any relaxation effects of the steel parts in the bolted joint are neglected. In figure 15a the static relaxation curves of AZ91 and AE44 of the first 10 hours are displayed. The initial bolt load value after tightening of AZ91 is significantly higher than the one of AE44. According to the simulation results in ABAQUS it can be assumed that plastic deformations of the thread flanks in the Mg-nut material occur during tightening. As a consequence the lower material strength of the alloy AE44 causes earlier plastifications and lower initial bolt load values.

After a rapid loss of bolt load due to embedding, there occurs a slight increase during heating up. This increase is caused by a thermal expansion coefficient mismatch between the steel bolt and the clamped parts. During the heat-up phase the clamped parts consisting of steel sleeve, steel load cell $(\alpha=11*10^{-6}/K)$ and Mg plate $(\alpha=26*10^{-6}/K)$ expand more than the steel bolt. As a consequence the bolt load rises. This thermal mismatch also causes the bolt load loss during cooling down. After reaching constant temperature there is no significant difference in relaxation rate between both alloys. AZ91 as well as AE44 exhibit high relaxation rates in the beginning which decrease gradually whereas the relaxation rate of AE44 reaches a value below the one of AZ91. This causes an intersection point at about 20 hours and significantly higher bolt load values at the end of the test after 90 hours.

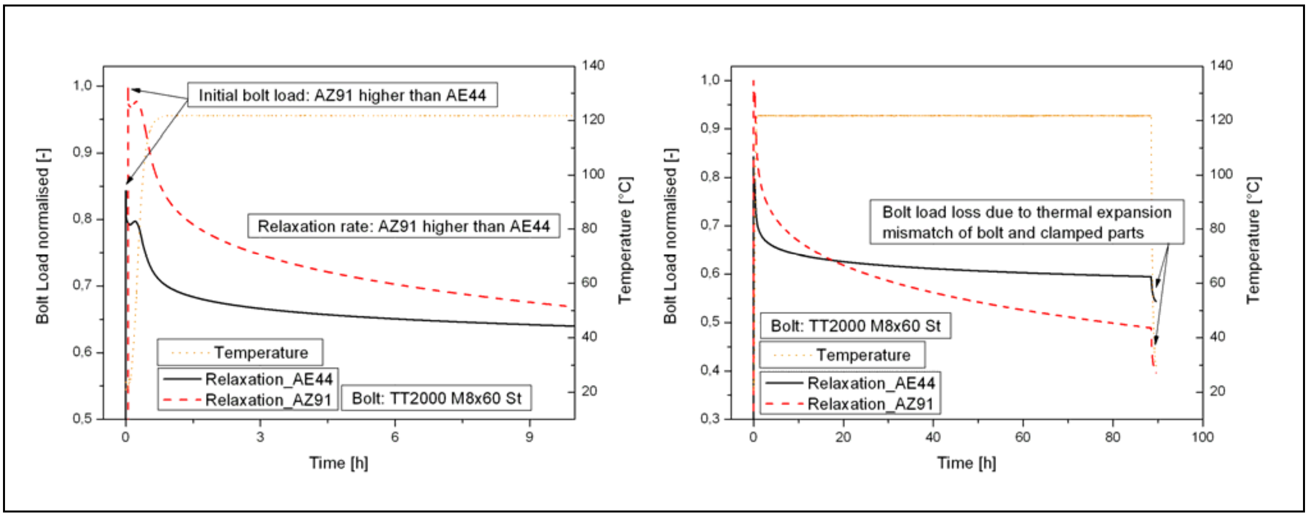

Figure 15: Experimental static relaxation tests of AZ91 and AE44 at 120°C for 10 hours (a), for 90 hours

When comparing the experimental relaxation tests of the bolted joint with the calculated relaxation curves out of creep test data, it can be seen that the qualitative correlation is good. As shown in the simulation, the initial values of the reaction force and the bolt load are different due to differing material strength of AZ91 and AE44. Furthermore, significantly lower minimum creep rates of AE44 lead to lower relaxation rates and to higher bolt load end values in comparison to AZ91. However, there is no visible difference in relaxation rate between both alloys immediately after tightening as may be expected because of simulation results.

Discussion and Conclusion

Experimental constant load creep tests revealed that a general preference of one alloy concerning creep resistance regardless of load and temperature level is not valid. Rather it has to be mentioned that AZ91 shows better creep performance for high loads whereas AE44 is superior for lower load levels. However, test results showed that for the temperature and stress ranges of interest for automobile applications the rare earth containing alloy AE44 has better creep strength than AZ91.

A possible explanation for this behaviour could be that at high load levels the thermally activated creep mechanisms are not predominantly critical for creep resistance due to short rupture times. Merely the basic material strength, which is higher for AZ91, influences the creep performance more strongly. On the contrary, test duration increases with decreasing loadings and the superior elevated temperature properties due to thermally stable precipitations Al_xRE_y in the microstructure of AE44 is the decisive factor of creep performance.

The pure magnesium relaxation calculations in ABAQUS show that different initial load values due to differing material strengths are to be expected. High primary creep rates of AE44 cause high relaxation rates immediately after load application. However, higher load end values occur according to lower minimum creep rates of AE44. In general the static relaxation test results show good correlation to simulation. Nevertheless, when comparing relaxation test results with simulation it is important to mention that there are still details missing which have to be taken into account. Firstly, creep tests were performed under uniaxial tensile loading whereas in the relaxation test, the Mg clamping part is loaded compressively. Secondly, in the thread flanks of the formed nut material is a multiaxial stress condition which depends on core hole size and tightening procedure whose influence on the creep and relaxation behaviour is not yet known.

References

[1] BUCH, F; SCHUMANN, S; FRIEDRICH, H et al (2002): New Die-Casting Alloy MRI153 for Power-Train Applications, Magnesium Technology

[2] DARGUSCH, M. S.; PETTERSON, K. & DUNLOP, G.L.: The Microstructure and Creep Behaviour of Die Cast Magnesium AZ91 and AS21 Alloys

[3] MORENO, I.P. et al (2003): Micro structural stability and creep of rare-earth containing magnesium alloys – Scripta Materialia 48: 1029-1034

[4] ZHU, S.M. et al (2008): Micro structural analysis of the creep resistance of die-cast Mg-4Al-2RE alloy – Scripta Materialia 58: 477-480

[5] EVANS, R.W. & WILSHIRE. B.(1985): Creep of Metals and Alloys, London, Institute of Metals

[6] DARGUSCH, M. S.; DUNLOP, G.L. & PETTERSON, K.: Elevated Temperature Creep and Microstructure of Die Cast Mg-Al Alloys: 277-282

[7] Dubbel, Taschenbuch für den Maschinenbau, 19. Auflage. Springer-Verlag Berlin, Heidelberg, New York 1997

[8] JAKOB, T.; GERSTMAYR, G.; LEITNER, H.; OBERHUBER, P. & HINTEREGGER, Chr.(2009): Cost and weight optimization of magnesium power train components by using aluminium thread forming fastener technology, SAE technical paper 2009-01-1256

[9] LEITNER, H.; HINTEREGGER, Chr.; JAKOB, T.; GERSTMAYR, G. & OBERHUBER, P. (2008): Einsatz hochfester Aluminium-Gewindefurchschrauben für Antriebsstrangkomponenten aus Magnesium-Legierungen zur Reduktion des Gewichtes und der Kosten, DVM-Bericht 675, DVM-Tag 2008 „Leichtbaustrategien“, Berlin